scattering. We expect a similar conclusion to hold whenever the magnetic-impurity scattering has an appreciable energy dependence within the range of $k_B T$. Any comparison between experiment and theory, although the latter may invoke a different effective relaxation time than (1), suffers therefore from the considerable complication that the magnitude of the mutual interference between the various scattering mechanisms would have to be determined from the Boltzmann equation, in order to assess what part of the measured total resistivity is due to magnetic impurities considered separately and what part is due to interference.

It is a pleasure to thank K. K. Murata for helpful discussions and C. A. Kukkonen for computational assistance.

---

*Work supported in part by the National Science Foundation under Grant No. GP-7198, in part by the Advanced Research Projects Agency through the Materials Science Center at Cornell University, MSC Report No. 1255, and in part by Statens Teknisk-Videnskabelige Fond, Denmark.

†Permanent address: Fysisk Laboratorium I, H. C. Ørsted Institutet, Copenhagen, Denmark.

‡Alfred P. Sloan Foundation Fellow.

[1]M. D. Daybell and W. A. Steyert, Phys. Rev. Letters 18, 398 (1967) (Cu:Fe), and 20, 195 (1968) (Cu:Cr).

[2]E. H. Sondheimer, Proc. Roy. Soc. (London), Ser. A 203, 75 (1950).

[3]See, for example, J. S. Dugdale and Z. S. Basinski, Phys. Rev. 157, 552 (1967).

[4]See, for example, Y. Nagaoka, Phys. Rev. 138, A1112 (1965); D. R. Hamann, Phys. Rev. 158, 570 (1967); Y. Nagaoka, Prog. Theor. Phys. 39, 533 (1968); K. K. Murata and J. W. Wilkins, in Proceedings of the Eleventh International Conference on Low Temperature Physics, St. Andrews, Scotland, 1968, edited by J. F. Allen, D. M. Finlayson, and D. M. McCall (St. Andrews University, St. Andrews, Scotland, 1969), p. 1242.

[5]M. J. Rice, Phys. Rev. Letters 23, 1108 (1969), has recently suggested that such interference effects may be the key to the understanding of the resistive anomalies of dilute alloys by demonstrating how changes in the low temperature electron-phonon resistivity may be related to the observed giant thermopower.

[5a]A considerably earlier treatment by C. A. Domenicali, Phys. Rev. 117, 984 (1960), using a more tractable, if less physical form for the scattering, arrived at similar results.

[6]H. Smith and J. W. Wilkins, to be published.

[7]A. H. Wilson, The Theory of Metals (Cambridge U. P., Cambridge, England, 1965), 2nd ed., p. 260.

[8]J. M. Ziman, Electrons and Phonons (Oxford U. P., Oxford, England, 1960), p. 275 ff; see also H. Højgaard Jensen, H. Smith, and J. W. Wilkins, Phys. Rev. 185, 323 (1969).

[9]H. Smith and J. W. Wilkins, Phys. Rev. 183, 624 (1969).

---

# REMARKS ON THE RENORMALIZATION OF LOCAL SPIN FLUCTUATIONS IN METALS

M. T. Béal-Monod*
Physique des Solides, Faculté des Sciences, Orsay, France

and

D. L. Mills†‡
Department of Physics, University of California, Irvine, California

(Received 8 December 1969)

By a perturbation-theoretic calculation, we find that vertex corrections make an important contribution to the renormalized spin-fluctuation temperature in dilute alloys, in the limit of strong local enhancement.

There has been a considerable amount of interest in locally enhanced spin fluctuations in nearly magnetic dilute alloys. Qualitative descriptions of this phenomenon have appeared that base the discussion on a random-phase-approximation (RPA) calculation of the dynamic susceptibility of the inhomogeneous system.[1] Attempts to treat this problem more rigorously have appeared,[2,3] because the RPA breaks down when the local enhancement is very strong. In these theories, one obtains a self-consistent renormalized one-electron propagator by including self-energy graphs known to be important in the region of strong local enhancement. But vertex corrections have not been included in these studies. In this note we point out that in the limit of strong local enhancement, vertex corrections to the $T = 0$ static susceptibility $\chi$ are equally or more important (in a sense defined below) than self-energy corrections. We feel that inclusion of vertex corrections in the theory may remove a number of difficulties with recent theories that have been

noted.[3]

We show the importance of vertex corrections by studying the dependence of diagrams that contain one, two, and three internal local paramagnon propagators on the local enhancement parameter

$$K_0^2 = \lim_{\omega\to 0}[1 - I\chi_{\mathrm{loc}}^{\mathrm{HF}}(\omega)]$$

where $I$ is the strength of the interaction between electrons in the impurity cell, and $\chi_{\mathrm{loc}}^{\mathrm{HF}}(\omega)$ is the local susceptibility of the single band of Bloch electrons. As the Hartree-Fock (HF) criterion for moment formation is approached by increasing $I$, then $K_0^2 \to 0$. We show that the terms containing one, two, and three local paramagnon lines contribute leading terms of order $\ln K_0^2$, $(\ln K_0^2)^2$, and $K_0^{-2}$ to the renormalized spin-fluctuation temperature

$$\tilde{T}_{sf} = E_F \lim_{\omega\to 0}[1 - I\tilde{\chi}_{\mathrm{loc}}^{\,i}(\omega)].$$

In this expression, $\tilde{\chi}_{\mathrm{loc}}^{\,i}(\omega)$ is a renormalized, irreducible[4] particle-hole bubble, to be discussed below. In each order we have examined, vertex corrections are comparable to or larger in magnitude than self-energy corrections, when $K_0^2 \ll 1$. Thus, vertex corrections must be included in the theory to obtain a proper description of the local spin-fluctuation theory, contrary to what was hoped.[3] We explore only the perturbation-theoretic calculation discussed above. We do not address ourselves to the problem of including vertex corrections in the theory in a complete, self-consistent fashion. We have attempted to sum the perturbation series. It appears difficult to sum the series in a meaningful way, as we shall see. More sophisticated methods might be needed to deal with this question.[5]

We study the transverse spin susceptibility $\chi$ of a nonmagnetic host containing a nearly magnetic impurity. Exchange enhancement in the host is ignored. A general formula for $\chi$ may be obtained by solving a set of coupled Bethe-Salpeter equations:

$$\begin{aligned}\tilde{\chi}(k=0,k=0) &= \tilde{\chi}^i(k=0,k=0) \\ &\quad + \tilde{\chi}^i(k=0,r=0) I \tilde{\chi}(r=0,k=0), \\ \tilde{\chi}(r=0,k=0) &= \tilde{\chi}^i(r=0,k=0) \\ &\quad + \tilde{\chi}^i(r=0,r=0) I \tilde{\chi}(r=0,k=0). \end{aligned} \quad (1)$$

The symbol $\tilde{\chi}(k=0,r=0)$ describes the total moment ($k=0$ Fourier component) induced in the system by a magnetic field applied locally to the impurity cell. The remaining quantities are defined in a similar fashion, and the superscript $i$ refers to an irreducible particle-hole propagator. For $\chi$ one then obtains

$$\chi = \tilde{\chi}(k=0,k=0) = \tilde{\chi}^i(k=0,k=0) + \frac{I\tilde{\chi}^i(k=0,r=0)^2}{1 - I\tilde{\chi}^i(r=0,r=0)}. \quad (2)$$

We refer below to the quantity $\tilde{\chi}^i(r=0,r=0)$ by the symbol $\tilde{\chi}_{\mathrm{loc}}^{\,i}$. Equation (2) is quite general. In the RPA it reduces to the expression[1] $\chi = \chi_{\mathrm{host}} + I\chi_{\mathrm{host}}^2/(1 - I\chi_{\mathrm{host}})$.

We will direct our discussion to the properties of $\tilde{\chi}_{\mathrm{loc}}^{\,i}$. The divergences we encounter will also appear in the other irreducible quantities in Eq. (2), but with different coefficients. It is the nature of the divergences that are of interest here since, as we shall see, we cannot sum the resulting series in a simple way. We also consider only the absolute zero of temperature. Recall that in the theory of uniformly enhanced systems,[6] higher-order paramagnon corrections lead to negligible changes in the $T=0$ susceptibility. In the local-enhancement problem, we find divergent contributions to $\chi$ at $T=0$, as $K_0^2 \to 0$.

To compute $\tilde{\chi}_{\mathrm{loc}}^{\,i}$, in principle we need to sum the infinite series of graphs obtained by dressing the bare bubble $\chi_{\mathrm{loc}}^{\mathrm{HF}}$ with all possible allowed insertions of internal paramagnon propagators (ladders or strings of an odd or even number of bubbles). The only difference between the diagrams considered here and those considered previously[7] is that we now have a local interaction, so wave vector is not conserved at the vertices. Thus, we can employ the formulas of Ref. 7 directly, but we replace $\chi^{(0)}(\vec{P},\omega)$ by $\chi_{\mathrm{loc}}^{\mathrm{HF}}(\omega) = \sum_{\vec{P}} \chi^{(0)}(\vec{P},\omega)$, and the electron propagator $G^{(0)}(\vec{k},\epsilon)$ by $\sum_{\vec{k}} G^{(0)}(\vec{k},\epsilon)$. With these rules in mind, we can proceed to calculate each diagram very much as for the uniform case, but note the effect of the above changes. We refer the reader to the appendix of Ref. 7 for the details of the uniform case. As an example, the diagram of Fig. 1(b) will give, for the local problem, the contribution $\chi_{1b}$ to $\tilde{\chi}_{\mathrm{loc}}^{\,i}$:

$$\chi_{1b} = T^2 \sum_{\epsilon,\omega} \chi_{\mathrm{even}}(\omega)[G^0(\epsilon)]^2[G^0(\epsilon+\omega)]^2, \quad (3)$$

where $\chi_{\mathrm{even}}(\omega)$ describes a string of an even number of bubbles:

$$\chi_{\mathrm{even}} = I^3[\chi_{\mathrm{loc}}^{\mathrm{HF}}(\omega)]^2/\{1 - [I\chi_{\mathrm{loc}}^{\mathrm{HF}}(\omega)]^2\}. \quad (4)$$

One has four diagrams of the form of Fig. 1(a). Two contain a string of an odd number of bubbles $[\chi_{odd}(\omega)]$ and two have ladder insertions $[\chi_{1ad}(\omega)]$. These diagrams give a contribution $\chi_{1a}$:

$$\chi_{1a}=2T^2\sum_{\epsilon,\omega}[\chi_{odd}(\omega)+\chi_{1ad}(\omega)]\times[G^0(\epsilon)]^3G^0(\epsilon+\omega), \quad (5)$$

where

$$\chi_{odd}(\omega)=-I^2\chi_{loc}{}^{HF}(\omega)/\{1-[I\chi_{loc}{}^{HF}(\omega)]^2\}, \quad (6)$$

and

$$\chi_{1ad}(\omega)=-I^2\chi_{loc}{}^{HF}(\omega)/[1-I\chi_{loc}{}^{HF}(\omega)]. \quad (7)$$

We consider only the limit of strong local enhancement, where

$$K_0{}^2=\lim_{\omega\to 0}[1-I\chi_{loc}{}^{HF}(\omega)]\ll 1.$$

The paramagnon propagators are then strongly peaked near $\omega=0$. Since the (unrenormalized) one-electron propagator $G^0(\epsilon)$ is a smooth function of energy, and varies appreciably only when $\epsilon$ changes by an amount the order of the bandwidth, we neglect the effect of the paramagnon energy transfer $\omega$ on $G^0(\epsilon)$, and replace $G^0(\epsilon+\omega)$ by $G^0(\epsilon)$. Equations (3) and (5) give

$$\chi_{1b}=T\sum_{\omega}\frac{I^3[\chi_{loc}{}^{HF}(\omega)]^2}{1-I^2[\chi_{loc}{}^{HF}(\omega)]^2}T\sum_{\epsilon}[G^0(\epsilon)]^4, \quad (8)$$

$$\chi_{1a}=2T\sum_{\omega}\frac{-I^2\chi_{loc}{}^{HF}(\omega)}{1-I^2[\chi_{loc}{}^{HF}(\omega)]^2}+\frac{-I^2\chi_{loc}{}^{HF}(\omega)}{1-I\chi_{loc}{}^{HF}(\omega)}T\sum_{\epsilon}[G^0(\epsilon)]^4. \quad (9)$$

Only diagrams of Fig. 1(a), which describe self-energy corrections to the single-particle propagator, are retained in Hamann's treatment[3] of the renormalization of the Anderson model. It is clear from Eq. (9) that the vertex corrections $\chi_{1b}$ of Fig. 1(b), which are not included in Hamann's treatment, are the same order in $K_0{}^2$ as the diagrams of Fig. 1(a), in the limit as $K_0{}^2\to 0$. At this point we see that one must consider the vertex corrections to obtain a complete description of locally enhanced systems, when $K_0{}^2\to 0$. We proceed by employing an approximate form for $I\chi_{loc}{}^{HF}(\omega)$ that will enable us to study the various contributions as $K_0{}^2\to 0$:

$$I\chi_{loc}{}^{HF}(\omega)\cong 1-K_0{}^2+i\lambda\omega\,\mathrm{sgn}(\mathrm{Im}(\omega)). \quad (10)$$

The sums over the paramagnon frequency $\omega$ may then be evaluated in the usual way. We find by this means that as $T\to 0$,

$$\chi_{1a}+\chi_{1b}=-\tfrac{5}{2}I\ln K_0{}^2\{T\textstyle\sum_{\epsilon}[G^0(\epsilon)]^4\}. \quad (11)$$

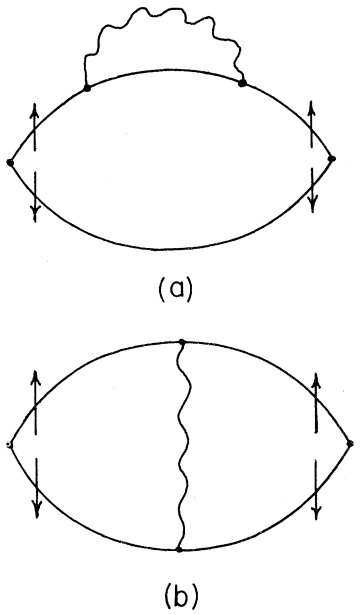


FIG. 1. The two classes of diagrams with one local paramagnon insertion. The local paramagnon propagator is denoted by a wiggly line.

For the one-paramagnon diagrams, the presence of the vertex correction of Fig. 1(b) changes the coefficient of the $\ln K_0{}^2$ term, but the form of the divergence does not change. One may see this by noticing that $\chi_{even}(\omega)$ of Eq. (3) combines with one of the $\chi_{odd}(\omega)$ of Eq. (5) [after we replace $G^0(\epsilon+\omega)$ by $G^0(\epsilon)$] to give a nondivergent quantity when $K_0{}^2\to 0$:

$$\chi_{even}(\omega)+\chi_{odd}(\omega)=-I^2\chi_{loc}{}^{HF}(\omega)/[1+I\chi_{loc}{}^{HF}(\omega)]. \quad (12)$$

We shall see that graphs with three paramagnon insertions will change the nature of the divergence.

In the later discussion, it will be convenient to note that

$$\chi_{1ad}(\omega)+\chi_{even}(\omega)=\chi_{odd}(\omega). \quad (13)$$

Next we examine diagrams involving two paramagnon insertions (Fig. 2). We first look at the vertex corrections of Fig. 2(a) and 2(b), since they involve $G^0(\epsilon)$ in the form $[T\sum_{\epsilon}G^0(\epsilon)^3]^2$, where all others involve $T\sum_{\epsilon}[G^0(\epsilon)]^6$. Moreover, from conservation of energy considerations, the two paramagnon propagators in Fig. 2(a) and 2(b) involve the same frequency, while the two propagators in each of the other graphs in Fig. 2 involve independent frequencies. The diagrams of Figs. 2(a) and 2(b) are drawn in detail in Ref. 7

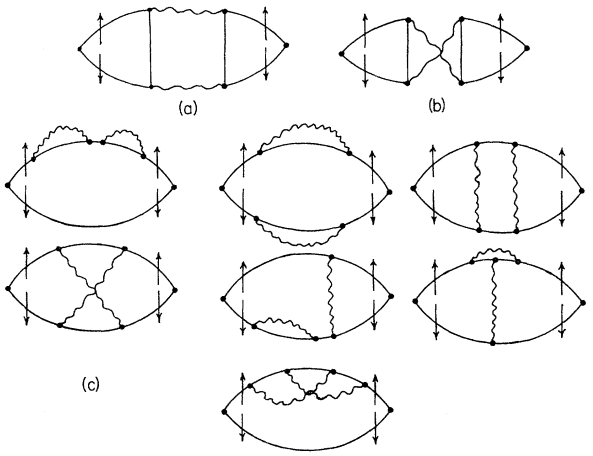


FIG. 2. Diagrams with two local paramagnon lines. Part (c) contains the seven graphs in the lower three lines.

One has

$$\chi_{2a}+\chi_{2b}=2T\sum_{\omega}\frac{-I^2}{1-[I\chi_{loc}{}^{HF}(\omega)]^2}\times T\{\textstyle\sum_{\epsilon}[G^0(\epsilon)]^3\}^2 \qquad (14)$$

where we have used Eq. (12). The sum over $\omega$ gives, as $T\to 0$,

$$\chi_{2a}+\chi_{2b}\propto -I^2\ln K_0{}^2[T\textstyle\sum_{\epsilon}G^0(\epsilon)^3]^2. \qquad (15)$$

These vertex corrections are not included in the work of Hamann, and they will change the coefficient of the $\ln K_0{}^2$ term. It is important to note that the dimensionless coupling constant of the present problem, $IN(0)$, where $N(0)$ is the density of states at the Fermi energy, is not small compared with unity. Thus, the contributions $\chi_{2a}$ and $\chi_{2b}$ to the $\ln K_0{}^2$ term are comparable in magnitude to those from the graphs with one paramagnon insertion.

The remaining diagrams of Fig. 2 contain both self-energy insertions and vertex corrections. These graphs may be computed by the methods described above, and the nature of the divergence as $K_0{}^2\to 0$ from the various graphs may be isolated. The calculations are straightforward, and we omit the details here. Upon employing Eqs. (12) and (13), one finds at $T=0$ contributions proportional to $\ln K_0{}^2\{T\sum_{\epsilon}[G^0(\epsilon)]^6\}$ as well as stronger divergences proportional to $(\ln K_0{}^2)^2\times\{T\sum_{\epsilon}[G^0(\epsilon)]^6\}$. At this point in the discussion, it is clear that vertex corrections give contributions to $\tilde{T}_{sf}$ of equal importance to the self-energy corrections. At the same time, the difficulty of isolating a subset of dominant graphs in each order is evident, as one can see from the discussion of the $\ln K_0{}^2$ terms.

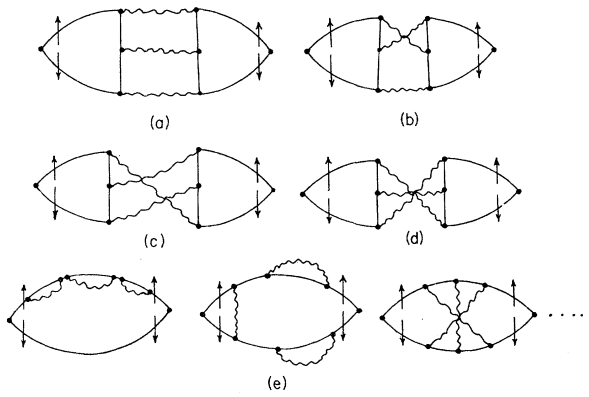


FIG. 3. Some of the diagrams with three local paramagnon lines.

We finally move to the graphs in Fig. 3 involving three local paramagnon insertions. We separate the diagrams of Figs. 3(a)-3(d) which involve $\{T\sum_{\epsilon}[G^0(\epsilon)]^4\}^2$ from those of Fig. 3(e) involving $T\sum_{\epsilon}[G^0(\epsilon)]^8$. From the graphs of Fig. 3(e), calculations along the lines of those above yield corrections proportional to $(\ln K_0{}^2)^3$, as well as lower powers of $\ln K_0{}^2$.

We now consider the terms in Figs. 3(a)-3(d), which we find give contributions of order $K_0{}^{-2}$, in contrast to the logarithmic divergences found in the lower orders. Inspection of these graphs shows that twenty distinct graphs are encountered: 18 contain one ladder and two strings of bubbles, while two involve ladders only (three parallel, and three crossed ladders). These graphs sum to

$$\chi_{3a\text{-}d}=\{T\textstyle\sum_{\epsilon}[G^0(\epsilon)]^4\}^2T^2[5\sum_{\omega,\omega'}\chi_{lad}(\omega)\chi_{odd}(\omega')\chi_{odd}(-\omega-\omega')+5\sum_{\omega,\omega'}\chi_{lad}(\omega)\chi_{even}(\omega')\chi_{even}(-\omega-\omega')$$
$$+8\sum_{\omega,\omega'}\chi_{lad}(\omega)\chi_{odd}(\omega')\chi_{even}(-\omega-\omega')+2\sum_{\omega,\omega'}\chi_{lad}(\omega)\chi_{lad}(\omega')\chi_{lad}(-\omega-\omega')]. \qquad (16)$$

We write this in a symbolic fashion:

$$\chi_{3a\text{-}d}=T^2\sum_{\omega,\omega'}(5\ \text{lad}\times\text{odd}\times\text{odd}+5\ \text{lad}\times\text{even}\times\text{even}+8\ \text{lad}\times\text{odd}\times\text{even}+2\ \text{lad}\times\text{lad}\times\text{lad}). \qquad (17)$$

Upon rearranging these terms, one finds

$$\{\cdots\} = 5 \text{ lad} \times (\text{odd} + \text{even}) \times (\text{odd} + \text{even}) + 2 \text{ lad} \times \text{lad} \times \text{lad} - 2 \text{ lad} \times \text{even} \times \text{even}, \tag{18}$$

$$\equiv \chi_{3a\text{-}d}{}^{(1)} + \chi_{3a\text{-}d}{}^{(2)} + \chi_{3a\text{-}d}{}^{(3)}. \tag{19}$$

One easily sees that $\chi_{3a\text{-}d}{}^{(1)}$ diverges like $T\sum_{\omega}\chi_{1ad}(\omega)$, i.e., like $\ln K_0{}^2$. The behavior of $\chi_{3a\text{-}d}{}^{(2)}$ and $\chi_{3a\text{-}d}{}^{(3)}$ is the same as that of

$$\chi_3' = T^2 \sum_{\omega,\omega'} [1 - I\chi_{1oc}{}^{HF}(\omega)]^{-1}[1 - I\chi_{1oc}{}^{HF}(\omega')]^{-1}[1 - I\chi_{1oc}{}^{HF}(-\omega-\omega')]^{-1}.$$

The sums on $\omega, \omega'$ may be converted from a sum over imaginary frequencies to an integral over real frequencies in the standard manner. Upon doing this, then using our approximate form for $\chi_{1oc}{}^{HF}(\omega)$ one gets

$$\chi_3' = \lambda^{-3} K_0{}^{-2} \mathcal{I},$$

where $\mathcal{I}$ is an integral over dimensionless quantities that converges in the absence of a frequency cutoff in $\mathrm{Im}(\chi_{1oc}{}^{HF}(\omega))$.

We see that as $K_0{}^2 \to 0$, $\chi_3'$, and hence the graphs with three paramagnon insertions, diverge as $K_0{}^{-2}$, in contrast to the logarithmic divergences encountered earlier. If only the self-energy corrections are retained in these third-order graphs, the divergent contributions are of order $(\ln K_0{}^2)^3$ or lower. This is the basis for our earlier statement that inclusion of vertex corrections in the theory may affect the functional dependence of $\tilde{T}_{sf}$ on $I$ in a qualitative manner. A theory that ignores these corrections appears to us to have limited validity.

It is unfortunate that we have been unable to isolate a single dominant set of graphs in each order that may then be summed to remove those divergences, and yield a closed expression for $\tilde{T}_{sf}$. One of the difficulties may be appreciated by recalling our earlier discussion of the $\ln K_0{}^2$ contribution to $\chi$; it appears that one obtains contributions to the coefficient of this term from graphs of all order in the local paramagnon propagator. Since the dimensionless parameter $IN(0)$ of the present problem is of order unity when $K_0{}^2 \ll 1$, the contributions to the $\ln K_0{}^2$ term from graphs second and higher order in the paramagnon propagator are comparable in magnitude to the terms with one paramagnon insertion. Thus, one apparently cannot isolate the most divergent term in $K_0{}^2$ in each order, and discard the less divergent terms in an attempt to sum the diagrams. We note that these remarks are similar to the comments of Silverstein and Duke[8] concerning the validity of low-temperature theories of the Kondo effect that are obtained by considering only the most divergent terms in each order of perturbation theory. But one important difference between the Kondo problem (discussed within the framework of the $s$-$d$ Hamiltonian) and the local enhancement problem is that in the former, a small dimensionless interaction parameter $JN(0)$ exists.

We wish to point out that Dr. S. K. Ma has made made useful contributions during the early stages of this work. We have also appreciated the helpful comments of D. R. Fredkin and P. Lederer. One of us (M.T.B.-M.) is grateful to H. Suhl for numerous discussions concerning various aspects of this problem.

*Laboratoire Associé au Centre National de la Recherche Scientifique.

†Research supported in part by the Office of Aerospace Research, U. S. Air Force Office of Scientific Research, under Grant No. AFOSR 68-1448.

‡Alfred P. Sloan Foundation Fellow.

[1]P. Lederer and D. L. Mills, Phys. Rev. 165, 837 (1968), and Phys. Rev. Letters 20, 1036 (1968); S. Engelsberg, W. F. Brinkman, and S. Doniach, Phys. Rev. Letters 20, 1040 (1968); N. Rivier and M. Zuckermann, Phys. Rev. Letters 21, 904 (1968).

[2]H. Suhl, Phys. Rev. Letters 19, 442 (1967); M. Levine and H. Suhl, Phys. Rev. 171, 567 (1968); M. Levine, T. V. Ramakrishnan, and R. A. Weiner, Phys. Rev. Letters 20, 1370 (1968).

[3]D. R. Hamann, Phys. Rev. (to be published).

[4]By irreducible bubble, we mean a diagram that cannot be separated into two pieces, each containing one external vertex, by cutting two electron lines at the ends of one interaction line.

[5]S. Wang, W. Evenson, and J. Schrieffer, Phys. Rev. Letters 23, 92 (1969).

[6]M. T. Béal-Monod, S. K. Ma, and D. Fredkin, Phys. Rev. Letters 20, 929 (1968).

[7]S. K. Ma, M. Béal-Monod, and D. Fredkin, Phys. Rev. 174, 227 (1968).

[8]C. B. Duke and S. D. Silverstein, J. Appl. Phys. 39, 708 (1968).